Fracture process zone size and energy dissipated during crack propagation in quasi-brittle materials

Ladislav Řoutil[1,a], Václav Veselý[1,b], Zbyněk Keršner[1,c], Stanislav Seitl[2,d] and Zdeněk Knésl[2,e]

[1] Institute of Structural Mechanics, Faculty of Civil Engineering, Brno University of Technology, Veveří 331/95, 602 00 Brno, Czech Republic

[2] Institute of Physics of Materials, Academy of Sciences of the Czech Republic, v.v.i.; Žižkova 22, 616 62 Brno, Czech Republic

[a] routil.l@ fce.vutbr.cz, [b] vesely.v1@fce.vutbr.cz, [c] kersner.z@fce.vutbr.cz, [d] seitl@ipm.cz, [e] knesl@ipm.cz

Keywords: cementitious composites, fracture energy, fracture process zone, numerical modelling

Abstract. The paper presents a numerical analysis of fracture processes in testing specimen configurations with substantially different crack tip stress constraint levels. Specimens of several sizes and relative notch lengths are taken into account. The features of the distribution of current/cumulative value of fracture energy along the specimen ligament are discussed and related to estimations of fracture process zone (FPZ) size and shape, in which the energy is dissipated. Significant effect of the stress constraint on the size/shape of the FPZ, and consequently the energy dissipated within it, is reported.

Introduction

Crack initiation and propagation in quasi-brittle materials/structures (e.g. structural members made of concrete and other cement-based composites) is preceded by the formation of a fracture process zone (FPZ). Quasi-brittle (tensile) failure can be modelled using cohesive crack models implemented in finite element method (FEM) codes. Fracture energy is an important parameter of these models. The best method of determining the fracture energy value is currently under debate because the value of the specific energy dissipated within the FPZ is not constant along the specimen's ligament during the fracture process. As a consequence, the value of fracture energy derived from the experiment is influenced by the size and geometry of the tested specimen.

This paper is focused on the development of the FPZ and the corresponding value of current and cumulative fracture energy dissipated within the FPZ during the fracture process at the crack tip in structural members which are characterized by different levels of stress constraint at the crack tip. The influence of the location, size and shape of the FPZ on the fracture energy value is studied using sets of numerical experiments. Three testing configurations of notched specimens with different constraint levels (see Table 1) were chosen for the parametric study, each set consisting of specimens of different size and different relative notch length. Current values of the fracture energy are assessed using a combination of the "work-of-fracture-method" and the equivalent elastic crack approach. This energy is evaluated at corresponding stages of the FPZ progress for each configuration, and other related effects are studied.

Evaluation of current and cumulative values of fracture energy, and estimation of the FPZ

The specific energy dissipated in an FPZ of a certain size and shape corresponding to the size, shape and boundary conditions of the specimen at a certain moment in the fracture process is marked as the current value of the fracture energy g_f [5]. Simultaneously, G_f is a cumulative (averaged) value of the instantaneous specific work of fracture dissipated from the beginning of the

Testing configuration	SEN-TPB	DEN-T	CN-T
	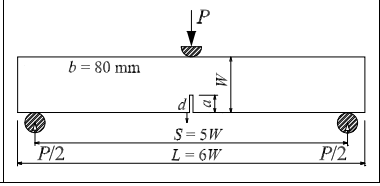	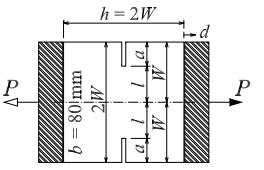	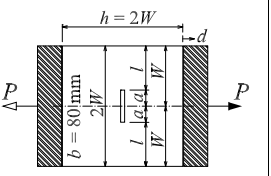
Specimen size $D = W$ (SEN-TPB) or $2W$ (DEN-T and CN-T) [mm] : 80, 160, 320, 640, 1280			
Relative notch length $\alpha_0 = a_0/W$ [-] : 0.1, 0.3, 0.5, 0.7, 0.85			

Table 1. Considered testing configurations, specimen sizes and relative notch lengths

fracture to a certain step. The RILEM value of fracture energy G_f^{RILEM}[10] is the averaged fracture energy of the fracture process through the entire specimen ligament. The distribution of g_f along the specimen ligament is not constant (a bilinear model for its approximation has been proposed – [3, 4]), which is the reason for the non-uniform distribution of the averaged fracture energy G_f^{RILEM} along the ligament, and in consequence for the dependence of this energy on the boundaries/geometry/size of the specimen [3, 4, 6, 7, 12]. Methods for the determination of "true" fracture energy, which should be independent of the geometry/size of the specimen, have been proposed recently [3, 4, 7]. However, these methods have been applied only on testing configurations with high stress constraint.

Fracture energy is defined as the energy needed for creating a crack surface of unit area. According to the "work-of-fracture method" [10], it is calculated from the whole load vs. the deflection curve (P–d diagram) recorded during the fracture test. For a specimen of width W, breadth b, with an initial crack of length a_0 (Tab. 1) the fracture energy is defined according to Eq. 1:

$$G_f^{RILEM} = \frac{1}{(W - a_0)b} \int P \, \mathrm{d}d \, . \tag{1}$$

The current value of the fracture energy g_f is the energy which dissipates in a FPZ of a certain size and shape that corresponds to the size, shape and boundary conditions of the specimen at a certain time point in the fracture process. It is derived from a work of fracture dissipated between two close-together steps in the fracture process (Fig. 1a), and its value for each time/fracture step i is defined according to Eq. 2 [13]:

$$g_{f,i} = \frac{1}{(\Delta a_i - \Delta a_{i-1})b} \left(W_{f,i} - W_{f,i-1} \right) , \tag{2}$$

where $W_{f,i}$ is referred to as a work of fracture according to the following formula:

$$W_{f,i} = \int_0^{d_i} P \mathrm{d}d - \frac{1}{2} P_i^2 C_i \, . \tag{3}$$

In this expression P denotes load, d means load-point displacement and $C=d/P$ is specimen compliance.

We can also define a cumulative value of fracture energy $G_{f,i}$ for each time (fracture) step i (Eq. 4, Fig. 1a).

$$G_{\mathrm{f},i} = \frac{W_{\mathrm{f},i}}{\Delta a_i b}. \tag{4}$$

In Eq. 2 and 4, $\Delta a_i = a_i - a_0$ means the equivalent elastic crack extension at time point i. The equivalent elastic crack extension Δa_i at that point was determined from secant specimen compliance according to the effective crack model [9]. The function of the geometry used in the procedure of calculating of Δa is limited (in this case by $0.02 \le \alpha \le 0.92$, due to large error out of this interval).

Note that at each point in the fracture process, the value of g_f is equal to the value of fracture resistance R calculated as $R = K_\mathrm{I}^\mathrm{e}/E$, where K_I^e is stress intensity factor at the equivalent elastic crack tip.

The above-mentioned approach – a combination of the "work-of-fracture-method" and the equivalent elastic crack model for the determination of progression of the cumulative value of the fracture energy G_f, and the current value of the fracture energy g_f during the fracture process [13] – were applied to three testing configurations of notched specimens with different constraint levels. The stress field around the crack tip can be described by means of two-parameter fracture mechanics, namely the stress intensity factor K and the T-stress [8]. The T-stress, equivalently the non-dimensional biaxiality factor $B = T\sqrt{\pi a}/K_\mathrm{I}$, is used for characterizing the constraint level. The shape and size of zone where given level of tension stress is exceeded for different values of T-stress is sketched in Fig. 1b. If the stress level is equal to tension strength the zone can be regarded as zone of failure (plastic zone in case of e.g. metallic materials [11]). The dependence of biaxiality factor B on relative crack length $\alpha = a/W$ for the studied geometries is displayed in Fig. 1c.

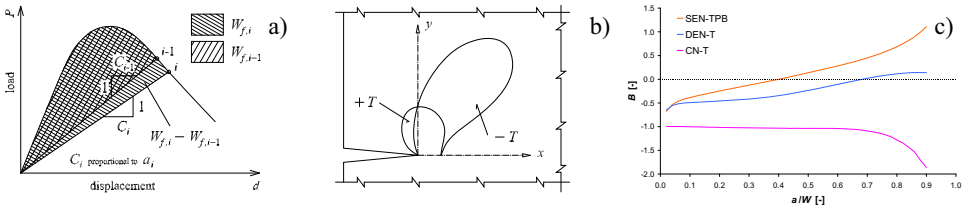

Fig. 1. a) Calculation of the current and cumulative work-of-fracture value from a P–d diagram, b) sketch of failure (plastic) zone shape for cases of high ($+T$) and low ($-T$) level of constraint, c) plot of biaxiality factor B vs. relative crack length $\alpha = a/W$ for the studied testing geometries

Numerical study

Description of analyses. Three already-mentioned testing configurations with different values of stress constraint at the crack tip (Tab. 1, Fig. 1c) were simulated using software ATENA 2D [1]: SEN-TPB (single-edge notched specimen in three point bending), DEN-T (double-edge notched specimen in tension), CN-T (centrally-notched specimen in tension). Five specimen sizes $D = W$ (80, 160, 320, 640, 1280 mm) and five values of relative notch length α_0 (0.1, 0.3, 0.5, 0.7, 0.85) were taken into account. Other specimen proportions were derived from W (Table 1). The analyses were conducted in a plane stress state with a fracture–plastic constitutive model. The fracture model is based on the classic orthotropic smeared crack formulation and crack band model, and employs the Rankine failure criterion and exponential softening [1]. The parameters of the material model were generated by the software for an input cubic compressive strength of concrete $f_\mathrm{cu} = 61$ MPa. The most important parameters of the fracture model that influence the fracture behaviour are tensile strength $f_\mathrm{t} = 3.719$ MPa, fracture energy $G_\mathrm{F}^\mathrm{FEM} = 92.98$ Jm^{-2} and the exponential type of softening traction–separation law with the crack opening at the complete release of stress $w_\mathrm{c} = 0.1285$ mm.

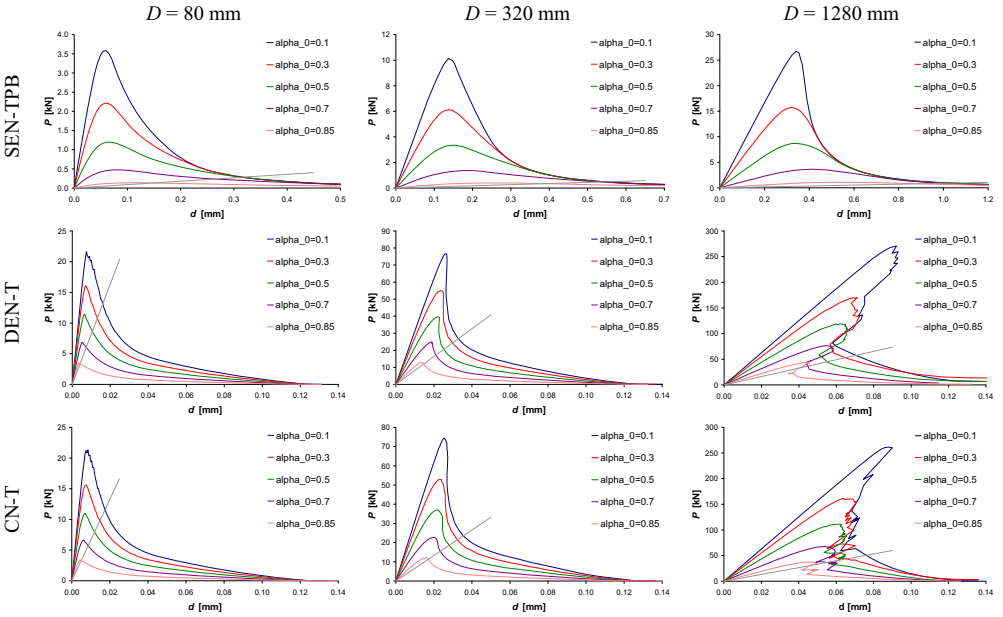

Fig. 2. Numerically simulated P–d diagrams for the three considered testing configurations (SEN-TPB, DEN-T, and CN-T) and three selected specimen sizes D (80, 320, and 1280 mm); compliances appropriate to relative crack length $\alpha = 0.92$ (grey line)

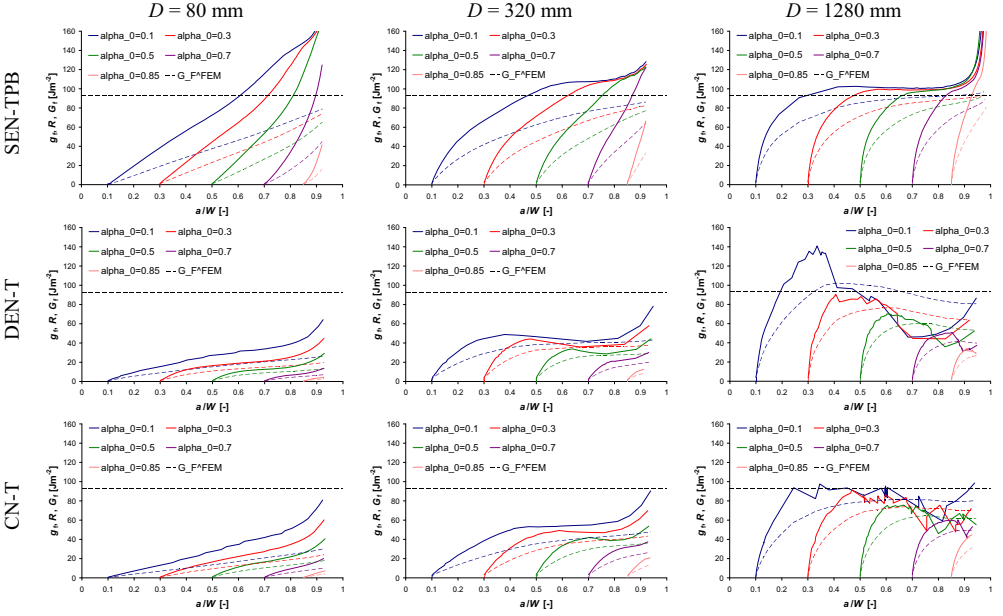

Fig. 3. Fracture energy progression (solid line – current value g_f (Eq. 2) = fracture resistance R, dashed line – cumulative value G_f (Eq. 4)) as functions of relative crack length (relative ligament length) corresponding to the P–d diagrams plotted in Fig. 2; the value of fracture energy used in the numerical model G_F^{FEM} (horizontal dashed line)

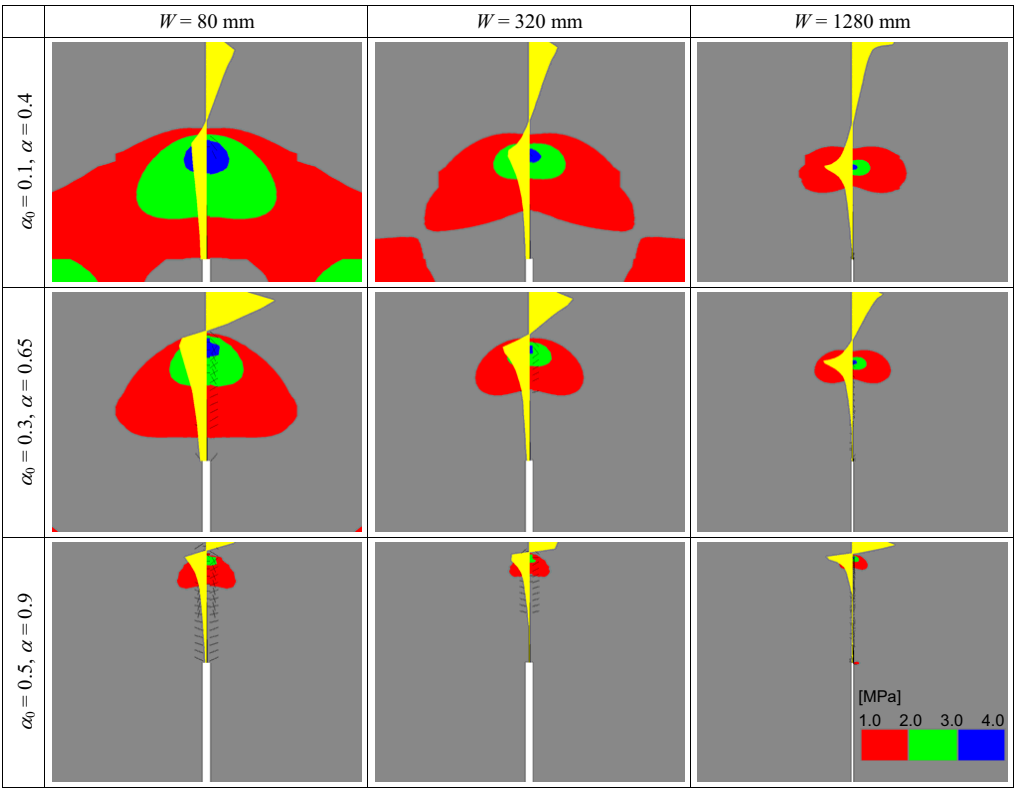

Fig. 4. Display of the chosen crack-opening stress isoareas and the profiles of the crack opening stress along the crack axis – SEN-TPB configuration for three specimen sizes D (80, 320, and 1280 mm) with three relative notch lengths α_0 (0.1, 0.3, and 0.5) at three stages of fracture process α (0.4, 0.65, and 0.9, respectively). Individual sections of Fig. 4 correspond to the middle part of specimens and the crack opening stresses along the crack axis are zoomed for this configuration

Obtained results – selected P–d diagrams, current and cumulative fracture energy progression, crack-opening stress isoareas and profiles of the crack opening stress along the crack axis – are displayed and described in Figs. 2–7.

Discussion of results – Current and cumulative values of the fracture energy approach the value of the fracture energy used in the simulations G_F^{FEM} for large specimens; this fact is obvious especially in the case of SEN-TPB testing configuration (Fig. 3). In other monitored configurations this approach is also closer when increasing the size of specimens, but this agreement is not absolute, especially in the cases of long notches. In that cases the divergences between G_F^{FEM} and courses of current and cumulative values of the fracture energy can be found. In Figs. 4, 5, and 6 the agreement in crack opening stress distribution (which influences the formation and extent of the FPZ) and courses of biaxiality factor B can be observed (compare these Figs. to Figs. 1b and c). In consequence, we can monitor the relation between the features of the FPZ (Figs. 3–7), which is influenced by the crack tip stress constraint, and the fracture energy consumption, which can be quantified by the current and cumulative values of the fracture energy g_f and G_f, respectively (Fig. 3).

In the case of the SEN-TPB configuration we can observe that the more constrained FPZ the more fracture energy is currently dissipating. This fact is true for all studied specimen sizes. For the

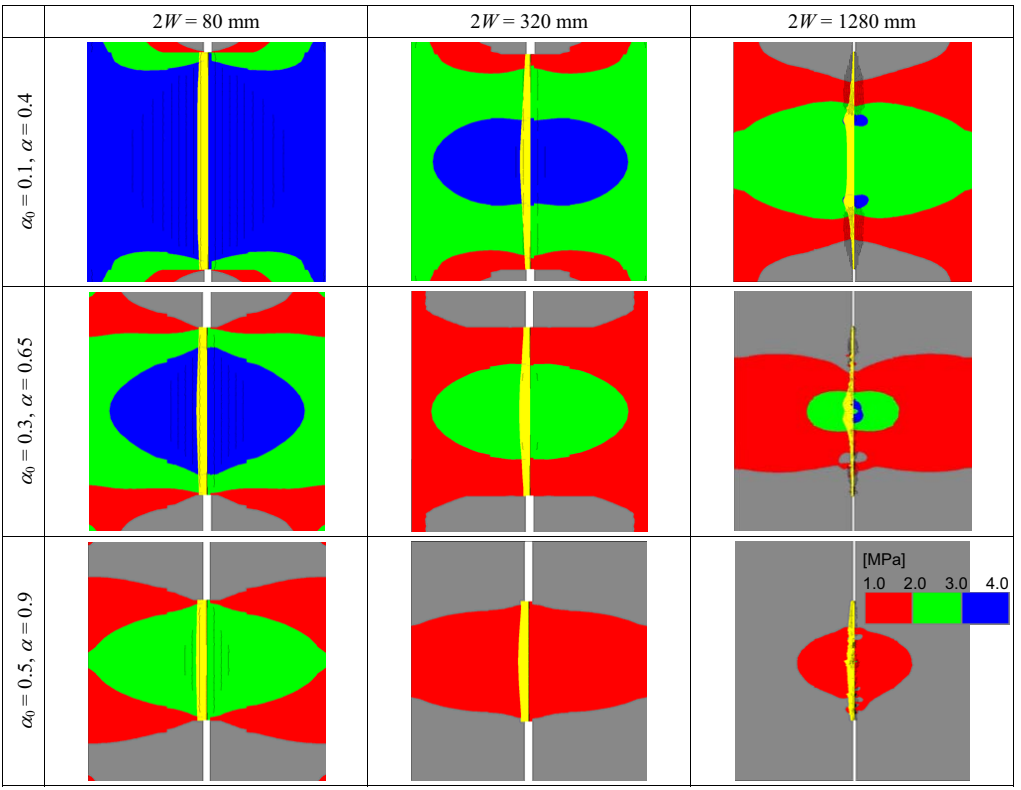

Fig. 5. The same as Fig. 4 – DEN-T configuration

DEN-T configuration we can notice that the consumptions of the current value of fracture energy decreases with increasing biaxiality factor for the large specimens. In the case of CN-T the course of the biaxiality factor is approximately constant until the relative crack length equal to 0.7 and we can observe very similar trend in the progression of the current value of the fracture energy for the large specimens. For the small specimens of both DEN-T and CN-T configurations the calculated fracture energy increases and its values of are much lower than the value G_F^{FEM} used in simulations.

Conclusions

Differences of FPZ size and shape for the individual investigated testing geometries characterized by different levels of crack tip stress constraint can be figured from the crack-opening stress isoareas and profiles depicted in Figs. 4, 5, 6 and 7. The different courses of the current/cumulative values of the fracture energy for the different specimen geometries and sizes can be related to these variances.

From the crack patterns displayed in the figures it is also apparent that the width of FPZ depends on the constraint level – the higher constraint the narrower FPZ and vice versa. From this fact it can be also concluded that the work of fracture method for the fracture energy determination, i.e. fracture energy defined as the work of fracture divided by the cracked ligament area, fails for geometries with low constraint, as has been shown in Fig. 3 for small DEN-T or CN-T specimens. In these cases the FPZ is rather wide so the fracture process takes place in relatively massive volume of the specimen. Therefore the specification of the energy dissipated in the volume by the area of the cracked ligament is reasonless.

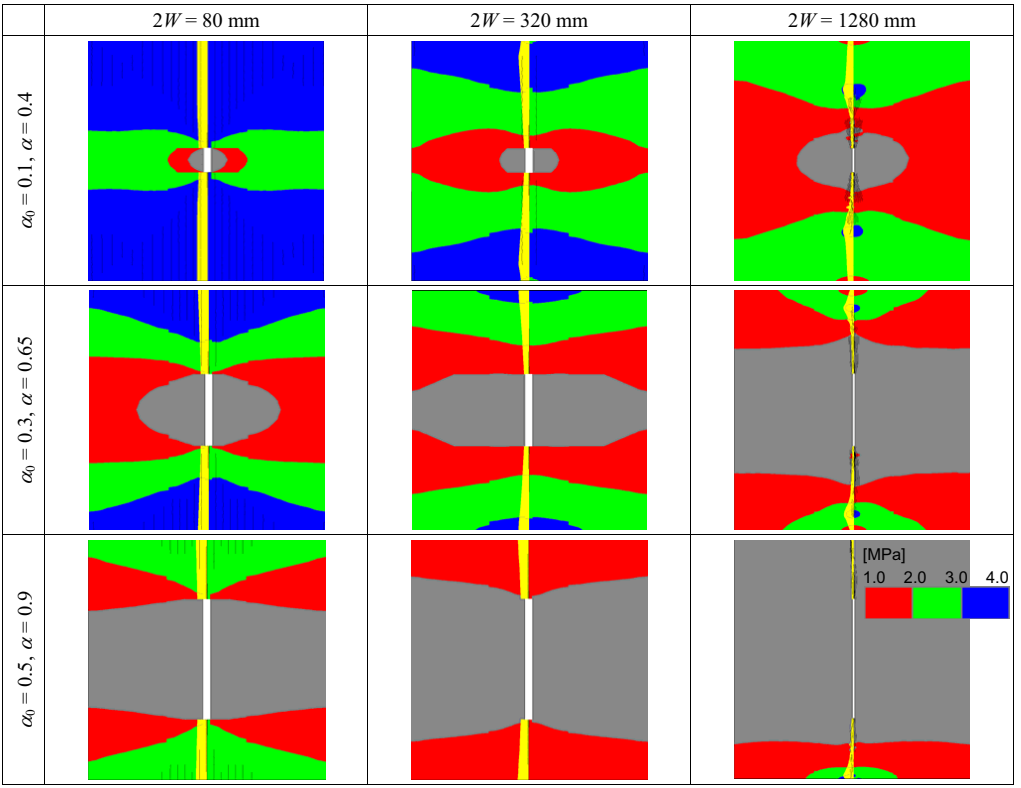

Fig. 6. The same as Fig. 4 and Fig. 5 – CN-T configuration

In case of SEN-TPB configuration (high constraint) the FPZ is narrow and with increasing of specimen size tends to a line and so the work of fracture method for evaluation of energy dissipated within it works quite well, especially for large specimens.

The analysis presented in this paper serves as a basis for development of testing and evaluation technique which should provide fracture characteristics of quasi-brittle materials independent (less dependent) on the specimen size, geometry and boundaries.

Acknowledgement

This outcome has been achieved with the financial support of the Ministry of Education, Youth and Sports, project No. 1M0579, within the activities of the CIDEAS research centre. In this undertaking, theoretical results gained in the project Grant Agency of Czech Republic 103/07/P403 were partially exploited.

References

[1] V. Červenka et al.: ATENA Program Documentation, Theory and Users manual for ATENA 2D (Cervenka Consulting, Prague 2003).

[2] Bažant, Z.P.: Analysis of work-of-fracture method for measuring fracture energy of concrete. Journ. Eng. Mech., 122(2) (1996) 138–144.

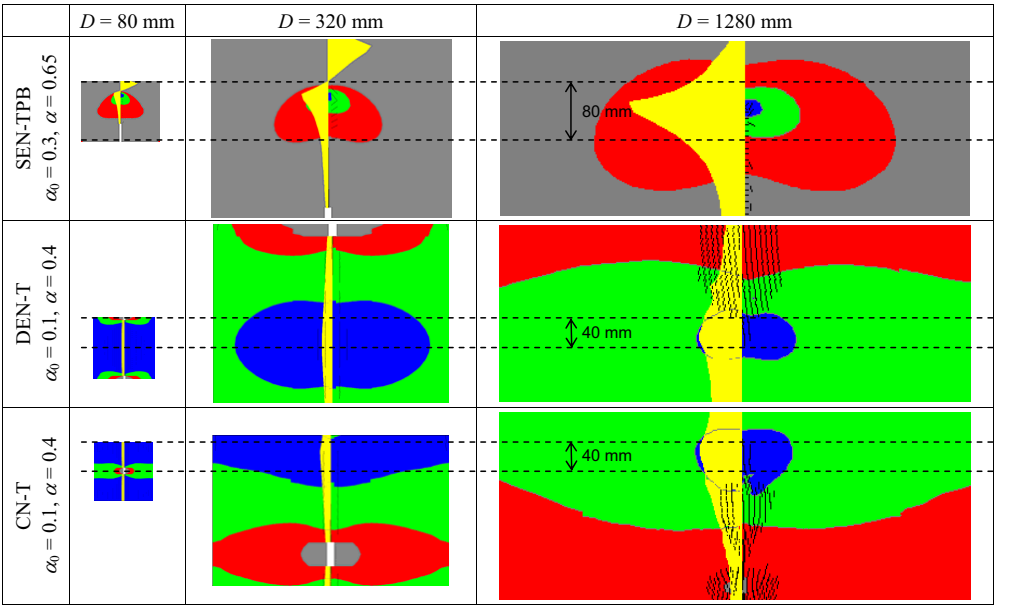

Fig. 7. Chosen crack-opening stress isoareas and profiles viewed in a corresponding length scale for selected specimen sizes and notch length at selected stages of fracture process

[3] K. Duan, X. Z. Hu and F. H. Wittmann: Explanation of size effect in concrete fracture using non-uniform energy distribution. Mater. Struct., Vol. 35 (2002), 326–331.

[4] K. Duan, X. Z. Hu and F. H, Wittmann: Boundary effect on concrete fracture and non-constant fracture energy distribution. Eng. Fract. Mech., Vol. 70 (2003), 2257–2268.

[5] X. Z. Hu and F. H. Wittmann: Fracture energy and fracture process zone. Mater. Struct., Vol. 25 (1992), 319–326.

[6] X. Z. Hu and K. Duan: Influence of fracture process zone height on fracture energy of concrete. Cem. Concr. Res., Vol. 34 (2004), 1321–1330.

[7] B. L. Karihaloo, H. M. Abdalla, and T. Imjai: A simple method for determining the true specific fracture energy of concrete. Mag. Concr. Res., Vol. 55 (2003), 471–481.

[8] Z. Knésl and K, Bednář: Two-parameter fracture mechanics: Calculation of parameters and its values (in Czech) (Institute of Physics of Materials, Czech Academy of Sciences, 1998).

[9] P. Nallathambi, P. and B. L. Karihaloo: Determination of specimen-size independent fracture toughness of plain concrete. Mag. Concr. Res., Vol. 38 (1986), 67–76.

[10] RILEM Committee FMC 50: Determination of the fracture energy of mortar and concrete by means of three-point bend test on notched beams. Mater. Struct., Vol. 18 (1985), 285–290.

[11] Suresh, S.: Fatigue of Materials. Cambridge: Cambridge University Press, 1998.

[12] B. Trunk, B. and F. H. Wittmann: Influence of size on fracture energy of concrete. Mater. Struct., Vol. 34 (2001), 260–265.

[13] V. Veselý, L. Řoutil, Z. Keršner: Structural geometry, fracture process zone and fracture energy. In *FraMCoS-6* (2007), London: Taylor & Francis Group, 111–118.